

Initial Cell Search and Selection for Load Balancing and Throughput Optimization in 5G Millimeter Wave Networks

Ning Wei, Xingqin Lin, Guangrong Yue, and Zhongpei Zhang

Abstract—The increasing adoption of the Internet of Things (IoT) requires careful design and optimization of the next-generation mobile networks (a.k.a. 5G) in every aspect to efficiently cope with the diverse and wide range of IoT requirements. Initial cell search and selection is one of the first few essential steps that a mobile device must perform to access a mobile network. The distinct features of 5G bring new challenges to the design of initial cell search and selection. In this paper, we propose a load aware initial cell search and selection scheme for 5G millimeter wave networks. The proposed scheme augments the existing pure received power based scheme by incorporating a new load factor broadcast as part of system information. We then formulate a throughput optimization problem using the optimal stopping theory. We characterize the throughput optimal stopping strategy and the attained maximum throughput. The results show that the proposed initial cell search and selection scheme is throughput optimal with a carefully optimized connection threshold.

I. INTRODUCTION

In June 2018, the third-generation partnership project (3GPP) approved the technical specifications for the standalone version of the 5th generation (5G) wireless access technology, known as new radio (NR) [1]. This milestone lays a solid foundation for the adoption of 5G NR for the Internet of Things (IoT). To facilitate the adoption of 5G in the IoT, further research in many technical aspects is needed to optimize 5G networks for better performance such as higher spectral and energy efficiency [2] and more efficient multiband spectrum sensing and resource allocation for IoT [3]. In this paper, we study initial cell search and selection in 5G millimeter wave networks to achieve better load balancing and optimized throughput performance.

A. Challenges of Initial Cell Search and Selection in 5G

In cellular networks, a user equipment (UE) needs to perform essential cell search and selection prior to data communication. Cell search usually involves two steps: 1) search and acquire synchronization to a cell, and 2) decode system

information that contains essential information for accessing the cell [4]. In initial cell search, the UE shall search for the strongest cell in long-term evolution (LTE) networks [5]. Once the UE finds an appropriate cell, it can select the cell and proceed to establish a connection with the cell by performing random access [6].

Although the received power based initial cell selection works well in single-tier homogeneous networks, it may result in unbalanced loads across the cells in multi-tier heterogeneous networks where the base stations (BSs) of small cells have much lower transmit powers than the BSs of macro cells [7], [8]. Further, millimeter wave (mmWave) is a distinct feature of 5G networks [1], [9]. MmWave communication utilizes the large chunks of spectrum resources in the millimeter wave bands (30-300 GHz) to achieve multi-Gbps data rates [10]. The load imbalance issue may become more serious in 5G networks where small cells would likely operate on the mmWave spectrum. If there were few connections in the mmWave small cells, the abundant radio resources brought by mmWave spectrum would not be sufficiently utilized.

One critical issue of mmWave communication is that their signals are susceptible to blockages [11], [12]. In particular, mmWave signals cannot penetrate many solid materials and even human body can attenuate the signals by as much as 20 to 35 dB [13]. This implies that mmWave connectivity will likely be highly intermittent, leading to probably much more frequent cell search and selection in 5G networks. Furthermore, mmWave communication requires beamforming to overcome the high pathloss as well as other losses due to rain and oxygen absorption and higher noise floor associated with larger bandwidth [10]. Therefore, beam searching and steering may have to be incorporated in the initial access procedures [14], [15]. The beam searching and steering process introduces additional non-negligible latency to the initial cell search and selection, due to the potentially large beam search space and the many cells and bands that need to be scanned.

B. Related Work

Due to the new challenges and complications of initial cell search and selection (or more generally, the initial access procedure) in 5G networks with mmWave communication, researchers and engineers are devoting significant efforts to the design of efficient protocols [14]–[21]. The work [14] proposes that BSs periodically transmit synchronization signals in random directions to scan the beam search space for

Ning Wei, Guangrong Yue, and Zhongpei Zhang are with the National Key Laboratory of Science and Technology on Communications, University of Electronic Science and Technology of China, Sichuan, China. (Email: wn, yuegr, zhangzp@uestc.edu.cn.)

Xingqin Lin is with Ericsson Research, Santa Clara, CA, USA. (Email: xingqin.lin@ericsson.com.)

This work was supported by National Natural Science Foundation of China (Grant No.'s 61871070, 61831004).

cell search, and is further extended in [15] to incorporate the random access procedure. In [16], the authors propose a two-step synchronization procedure, where in the first step UE obtains time and frequency synchronization by searching for the omni-directional synchronization signals from macro BSs and then in the second step determines the spatial directions by searching the directional synchronization signals from small BSs. The work [17] explores beamforming tradeoffs for initial UE discovery by adapting limited feedback-type directional codebooks. Several recently proposed initial cell search techniques including exhaustive and iterative search are surveyed and compared in [18]. In [19], the authors consider directional cell search in self-organized beam assignment in mmWave 5G networks and verify the proposed approach with simulations results in a realistic Manhattan environment. To improve the directional cell discovery process, the work [20] proposes to leverage context information related to user positions. Using tools from stochastic geometry, the authors of [21] conduct a system-wide performance analysis for initial access in a mmWave cellular system.

The aforementioned works on initial cell search and selection for mmWave networks are focused on beam searching and steering. In particular, they pay little attention to the load imbalance issue associated with the received power based cell selection schemes. In contrast, the load imbalance issue has drawn much attention in the context of heterogeneous networks without mmWave communication, and has led to many recent works on load balancing techniques [7], [22]. A suboptimal yet powerful load balancing approach called *biasing* has been proposed [23]. Biasing allows the low power BSs to artificially increase their transmit powers, and thus helps expand the coverage areas of small cells, making more UEs select and connect to small cells. Assuming a fully loaded model, the work [24] optimizes UE-BS association from a global network perspective. From a UE centric perspective, the work [25] formulates a network selection game and studies its dynamics. The proposed schemes in [24], [25], either centralized or distributed, require heavy signaling for information exchange between BSs and UEs. As a result, though the proposed schemes may be of interest in theory, it might be difficult to adopt them in practice, especially at the stage of initial cell search and selection. Furthermore, the existing works [7], [22], [24], [25] do not take into account the distinct features of mmWave communication in 5G networks, which as aforementioned introduces additional challenges and complications to the issue at hand. More recently, the work [26] considers joint load balancing and interference mitigation problem subject to wireless backhaul constraints in 5G heterogeneous networks, but it does not address the initial cell search problem.

In this paper, we propose a load aware initial cell search and selection scheme and apply optimal stopping theory to analyze the proposed scheme. Optimal stopping theory is about determining a time to take a given action based on causal observations to maximize an expected reward [27], [28]. The application of optimal stopping theory to wireless communications and networking can be found in a diverse set of problems [29]–[38]. For example, the early work [29]

applies optimal stopping theory to study joint probing and transmission strategies to maximize the system throughput in a broadcast fading channel. More recently, optimal stopping theory has been used to study emerging problems in the areas such as mmWave cellular systems [36], energy harvesting based wireless networks [37], coexistence of heterogeneous networks in TV white space [38], and cellular in unlicensed spectrum [39].

C. Main Outcomes and Contributions

In this paper, we study initial cell search and selection in 5G networks. We propose a load aware initial cell search and selection scheme to achieve a more balanced load distribution in 5G networks. In the proposed scheme, cell load information is included in the broadcast system information to facilitate initial cell search and selection. The proposed scheme augments the existing pure received power based initial cell search and selection scheme with a new load factor broadcast as part of the system information. This equips the networks with a powerful access control method that facilitates load balancing.

We then study the theoretical performance of the proposed initial cell search and selection scheme. We formulate a throughput optimization problem. Using the optimal stopping theory [27], [28], we cast the problem as a maximal rate of return problem. We characterize the throughput optimal stopping strategy and the attained maximum throughput. The results show that the proposed initial cell search and selection scheme is throughput optimal with a carefully optimized connection threshold. The optimal connection threshold and maximum throughput can be found by solving a fixed point equation. The fixed point equation in general does not admit a closed-form solution. We further provide an alternative characterization of the optimal throughput and use it to develop an iterative algorithm to compute the solution to the fixed point equation. We also prove the convergence of the proposed iterative algorithm.

II. PROPOSED INITIAL CELL SEARCH AND SELECTION

To achieve a more balanced load distribution in 5G networks, we propose that some cell load information is included in the broadcast system information to facilitate initial cell search and selection. Such load information may take various forms such as the number of connections in the cell, the available bandwidth, or the expected scheduling probability. To reduce access latency, the load information shall be broadcast in the first system information block. Such system information block usually consists of a limited number of important bits that shall be read by all the UEs before accessing the cell.¹

For concreteness, we assume that each cell i broadcasts the expected scheduling probability $\beta_i \in [0, 1]$ to control UE access. In other words, β_i would be treated by UE in the initial cell search and selection as the expected scheduling probability if the UE camps on the cell. The proposed expected scheduling probability may be considered as “soft” access barring. Access

¹In LTE, the first system information block is known as master information block (MIB) [4].

barring has been used in cellular networks including LTE to reduce the access load in case of an overload situation [40]. Compared to the existing access barring that takes a boolean value (i.e., access allowed or denied), the proposed expected scheduling probability takes value in $[0, 1]$ and thus is a soft access barring scheme.

We are now in a position to describe the proposed initial cell search and selection scheme. When examining a cell i , UE first obtains synchronization and measures the corresponding received signal-to-noise ratio (SNR) from the BS. If the measured received SNR from BS i (denoted as SNR_i) is below some threshold Γ , UE stops examining the current cell i and starts to examine another cell. Here, the threshold Γ is introduced to avoid selecting a cell with a too low SNR that may lead to poor link quality. If $\text{SNR}_i \geq \Gamma$, UE proceeds with decoding the first system information block to extract the cell load information, i.e., the expected scheduling probability β_i . Then UE computes the selection metric denoted as R_i as follows:

$$R_i = \beta_i \log(1 + \text{SNR}_i). \quad (1)$$

If R_i is greater than or equal to some connection threshold μ , UE selects the cell i and completes the cell search and selection process. Otherwise, UE repeats the process with another cell.

The proposed initial cell search and selection scheme is simple yet powerful. It augments the existing pure received power based scheme with a new load factor broadcast as part of the system information. It is up to the BS to decide and broadcast the value of the load factor, i.e., the expected scheduling probability β_i . For example, assuming that the number of active UEs served by BS i is M_i , a UE in the initial cell search may expect its scheduling probability to be $1/(M_i + 1)$ if it selects BS i as its serving cell. Therefore, the value of β_i broadcast by BS i may be chosen to be $1/(M_i + 1)$.

As an illustration example, Figure 1 shows a realization of load distribution under different association schemes in a two-tier network. In the network, a macro BS is located at the center (0, 0) m, four micro mmWave BSs are respectively located at (100, 100) m, (-100, 100) m, (-100, -100) m, and (100, -100) m, and 100 UEs are uniformly distributed. The macro BS operates in the 2 GHz band with 20 MHz carrier bandwidth, and the four micro mmWave BSs operate in the 39 GHz band with 1 GHz carrier bandwidth. The transmit powers of the macro BS and the micro BSs are respectively 46 dBm and 23 dBm. A total 30 dB beamforming gain is assumed for each mmWave link. The noise power spectral density is -174 dBm/Hz. The UE noise figure is 9 dB. The pathloss of each link is equal to $20 \log_{10} \left(\frac{4\pi}{\varrho} \right) + \alpha \cdot 10 \log_{10}(d)$ dB, where ϱ is the wavelength, $\alpha = 3.8$ is the pathloss factor, and d is the length of the radio link. Each link is also subject to a random log-normal shadowing with 7 dB standard deviation.

Figure 1(a) shows the load distribution under max-received-power association. The number of UEs selecting the macro BS is 76, while the numbers of UEs selecting the four micro BSs are 5, 4, 6, and 9, respectively. Figure 1(b) shows the load distribution under max-SNR association. Due to the high

noise floor associated with the large mmWave bandwidth, the numbers of UEs selecting the four micro BSs become even fewer. Specifically, in Figure 1(b), the number of UEs selecting the macro BS is 97, while the numbers of UEs selecting the four micro BSs are 1, 1, 0, and 1, respectively. Figure 1(c) shows the load distribution under the proposed max-selection-metric association, with the selection metric defined in (1). In this simulation, the value of β_i broadcast by BS i is equal to $1/(M_i + 1)$. Initially, $M_i = 0$. UE performs cell selection one by one. If a UE selects BS i , M_i is incremented by 1, and β_i is updated accordingly. For the purpose of illustration, the SNR threshold Γ is set to be $-\infty$, and the connection threshold μ of each UE is chosen such that each UE selects the BS that yields the maximum value of the selection metric for the UE. In Figure 1(c), the number of UEs selecting the macro BS is 25, while the numbers of UEs selecting the four micro BSs are 21, 15, 20, and 19, respectively. Clearly, compared to the load distribution in Figure 1(a) or Figure 1(b), this is a much more balanced load distribution that sufficiently utilizes the abundant radio resources brought by the mmWave spectrum.

This proposed scheme equips the networks with a powerful access control method that facilitates load balancing. Further, as will be shown later, the proposed scheme is throughput optimal with a carefully selected connection threshold μ . Note that it is also up to the BS to schedule the radio resources for each connected UE. In particular, the actual scheduling probability or the allocated radio resources of a UE can deviate from the expected scheduling probability broadcast as part of the system information.

III. SYSTEM MODEL AND PROBLEM FORMULATION

In this section, we describe a system model and formulate a throughput optimization problem for the initial cell search and selection scheme proposed in Section II.

A. Synchronization

In 5G networks that may operate on the mmWave spectrum, UE needs to determine the transmit spatial signature of a candidate BS and its corresponding receive spatial signature. Similar to [15], [21], we assume that UE learns the beamforming directions by detecting synchronization signals. Specifically, BSs periodically broadcast known synchronization signals with a period of T_{syn} seconds. To enable the detection of beamforming directions, each BS cycles through its set of transmit spatial signatures, and each UE also cycles through its set of receive spatial signatures. In a nutshell, denoting by L the number of possible transmit-receive spatial signature pairs, each beamforming scan cycle takes LT_{syn} seconds.

The described synchronization model is general and flexible [15]. For example, assume that each BS and each UE are equipped with an antenna array with N_{bs} antennas and N_{ue} antennas, respectively. Accordingly, N_{bs} and N_{ue} orthogonal beamspace directions are available at the BS and the UE, respectively. If both the BS and the UE scan over all the orthogonal beamspace directions, $L = N_{\text{bs}}N_{\text{ue}}$. If the BS scans over all the orthogonal beamspace directions but the UE uses an omni-directional or fixed antenna pattern, $L = N_{\text{bs}}$. On the

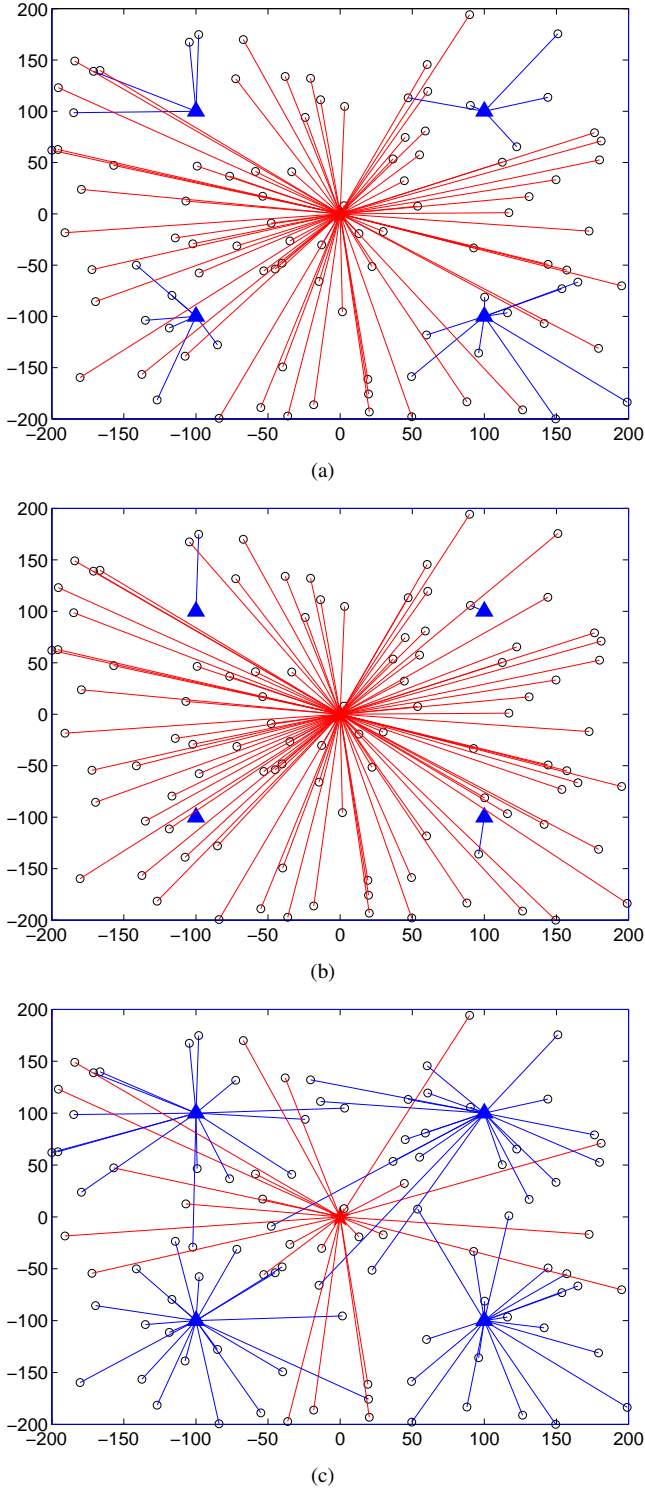


Fig. 1. A realization of load distribution under different associations in a two-tier network: max-received-power association in Figure 1(a); max-SNR association in Figure 1(b); max-selection-metric association in Figure 1(c).

contrary, $L = N_{\text{ue}}$ if the UE scans over all the orthogonal beamspace directions but the BS uses an omni-directional or fixed antenna pattern. If both the BS and the UE use omni-directional or fixed antenna patterns, $L = 1$.

Synchronization channels are usually designed to enable high detection rate at very low SNR. Therefore, for simplicity

we assume that each UE is able to obtain synchronization and determine the beamforming directions after a beamforming scan cycle.

B. Extracting Cell Load Information

We assume that BSs periodically broadcast the system information block containing cell load information with a period of T_{sib} seconds. Without loss of generality, we assume $T_{\text{sib}} \geq T_{\text{syn}}$; the analysis in this paper can be straightforwardly extended to the case $T_{\text{sib}} < T_{\text{syn}}$. The period T_{sib} is further chosen such that $T_{\text{sib}}/T_{\text{syn}}$ is an integer, facilitating the alignment of synchronization signals and system information broadcast channels. In particular, each system information broadcast channel can be positioned right after a synchronization signal. This minimizes the waiting time between a synchronization signal and a system information broadcast channel, leading to reduced latency of initial cell search and selection.

Similar to synchronization channels, system information broadcast channels are usually designed to cover UEs with low SNR. Therefore, for simplicity we assume that each UE is able to decode the system information block and extract cell load information in one shot.

C. Random Access Procedure and Data Communication

After UE finishes initial cell search and selection, it can initiate the random access procedure by transmitting a random access preamble to the selected BS. Once the random access procedure is completed, a connection between the UE and the BS is established, after which data communication may be scheduled.

We assume for simplicity that the random access procedure takes a fixed time of T_{ra} seconds. We focus on downlink data communication and assume that it lasts for a time duration of T_{data} seconds.

D. Problem Formulation

Consider a full communication period, during which a UE searches for n cells in the initial cell search and then selects a cell for the random access and data communication. Let T_n be the duration of the period. It follows that

$$T_n = \sum_{i=1}^n (Y_i + (L-1)T_{\text{syn}} + Z_i \mathbb{I}(\text{SNR}_i \geq \Gamma)) + T_{\text{ra}} + T_{\text{data}}, \quad (2)$$

where Y_i denotes the duration between the time instant that UE starts searching for cell i and the time instant that UE finds the first synchronization signal of cell i , and Z_i denotes the duration between the time instant that UE finishes synchronization for cell i and the time instant that UE decodes the system information broadcast channel of cell i .

We assume that the selection metrics $\{R_i\}$ defined in (1) are independent and identically distributed (i.i.d.). Denote by R the generic random variable for $\{R_i\}$ with cumulative distribution function $F_R(x)$. We further assume that the second moment of R exists. After searching n cells, the UE may select the best cell for the data communication. Accordingly,

UE may expect that the amount of downlink bits that it can receive equals

$$U_n = WT_{\text{data}} \max_{i=1, \dots, n} R_i \mathbb{I}(\text{SNR}_i \geq \Gamma), \quad (3)$$

where W denotes the channel bandwidth. Searching for more cells increases the probability of finding a better cell, since U_n is monotonically increasing with n . However, increasing the number n of searched cells also increases the duration of the overall communication period T_n . The tradeoff naturally raises the question: How many cells should the UE search before it stops searching and starts the random access procedure and data communication?

If the same cell search and selection rule is used across m communication periods, the total number of downlink bits that the UE can receive equals $\sum_{k=1}^m U_{n(k)}$, where $n(k)$ denotes the number of cells searched in the k -th period. Accordingly, the duration of the m periods equals $\sum_{k=1}^m T_{n(k)}$. Therefore, the throughput (bit/s) equals $\sum_{k=1}^m U_{n(k)} / \sum_{k=1}^m T_{n(k)}$. Letting $m \rightarrow \infty$, by the law of large numbers, the ergodic throughput equals $\mathbb{E}[U_N] / \mathbb{E}[T_N]$.

Denoting the set of admissible cell search and selection rules by

$$\mathcal{C} = \{N \in \mathbb{N}^+ : \mathbb{E}[T_N] < +\infty\}, \quad (4)$$

our objective is to find an optimal stopping rule N^* under the proposed cell search and selection scheme to obtain the maximum ergodic throughput λ^* . Mathematically, the throughput optimization problem is written as follows:

$$\lambda^* \triangleq \sup_{N \in \mathcal{C}} \frac{\mathbb{E}[U_N]}{\mathbb{E}[T_N]}. \quad (5)$$

IV. THROUGHPUT OPTIMAL STOPPING OF INITIAL CELL SEARCH AND SELECTION

A. Threshold Policy Achieves the Optimal Throughput

In this section, we characterize the throughput optimal stopping strategy N^* and the attained maximum throughput λ^* . To this end, we first derive the expected duration of a typical communication period in Lemma 1.

Lemma 1. *The expected duration $\mathbb{E}[T_n]$ of a communication period with n searched cells is given by*

$$\begin{aligned} \mathbb{E}[T_n] = & n \left(L - \frac{1}{2} \right) T_{\text{syn}} + \frac{n}{2} (T_{\text{sib}} - T_{\text{syn}}) \mathbb{P}(\text{SNR} \geq \Gamma) \\ & + T_{\text{ra}} + T_{\text{data}}. \end{aligned} \quad (6)$$

Proof. By the expression (2) of T_n and the linearity of expectation, we have that

$$\begin{aligned} \mathbb{E}[T_n] &= \sum_{i=1}^n (\mathbb{E}[Y_i] + (L-1)T_{\text{syn}} + \mathbb{E}[Z_i \mathbb{I}(\text{SNR}_i \geq \Gamma)]) \\ &\quad + T_{\text{ra}} + T_{\text{data}} \\ &= n(L-1)T_{\text{syn}} + \sum_{i=1}^n (\mathbb{E}[Y_i] + \mathbb{E}[Z_i] \mathbb{P}[\text{SNR}_i \geq \Gamma]) \\ &\quad + T_{\text{ra}} + T_{\text{data}}, \end{aligned} \quad (7)$$

where in the last equality we have used the fact that Z_i and SNR_i are independent. By the assumptions in Section III-A, it is clear that

$$\mathbb{E}[Y_i] = \frac{T_{\text{syn}}}{2}, \quad \forall i = 1, \dots, n. \quad (8)$$

By the assumption in Section III-B, we have that

$$\mathbb{P}(Z_i = jT_{\text{syn}}) = \frac{T_{\text{syn}}}{T_{\text{sib}}}, \quad j = 0, \dots, \frac{T_{\text{sib}}}{T_{\text{syn}}} - 1. \quad (9)$$

It follows that

$$\mathbb{E}[Z_i] = \frac{T_{\text{sib}} - T_{\text{syn}}}{2}, \quad \forall i = 1, \dots, n. \quad (10)$$

Plugging (8) and (10) into (7) yields (6). \square

While Lemma 1 characterizes the expected duration of a communication period, during which the UE searches n cells and selects a cell for the random access and data communication, different stopping rules yield different numbers of searched cells that possibly vary across communication periods. With Lemma 1, we are now in a position to derive the optimal stopping rule in Proposition 1.

Proposition 1. *The optimal stopping rule for the throughput maximization problem (5) is given by*

$$N^* = \min \{n \geq 1 : U_n \geq \lambda^*(T_{\text{ra}} + T_{\text{data}})\}, \quad (11)$$

where λ^* is the unique maximum throughput. Further, λ^* is the solution to the following fixed point equation:

$$\begin{aligned} \mathbb{E}[(U_n - \lambda(T_{\text{ra}} + T_{\text{data}}))^+] \\ = \lambda \left((L - \frac{1}{2})T_{\text{syn}} + \frac{T_{\text{sib}} - T_{\text{syn}}}{2} \mathbb{P}(\text{SNR}_n \geq \Gamma) \right), \end{aligned} \quad (12)$$

where $(x)^+ \triangleq \max(x, 0)$.

Proof. We first solve the associated ordinary optimal stopping problem:

$$V(\lambda) \triangleq \sup_{N \in \mathcal{C}} \mathbb{E}[U_N - \lambda T_N], \quad (13)$$

where λ is an arbitrary positive number. The duration of searching for cell 1 equals $Y_1 + (L-1)T_{\text{syn}} + Z_1 \mathbb{I}(\text{SNR}_1 \geq \Gamma)$. If the UE stops searching and selects cell 1 for the random access and data communication, it can receive $U_1 = R_1 \mathbb{I}(\text{SNR}_1 \geq \Gamma)$ information bits. If instead the UE continues to search for more cells from this point, the U_1 bits are not transmitted and the time $Y_1 + (L-1)T_{\text{syn}} + Z_1 \mathbb{I}(\text{SNR}_1 \geq \Gamma)$ has passed. In the search of cell 2, the problem starts over again, implying that the problem is invariant in time. Generalizing this to stage n , if the UE stops searching and selects the best cell from the n searched cells for the random access and data communication, it obtains a utility of $U_n - \lambda T_n$. If the UE continues to search for more cells, it obtains a utility of $V(\lambda) - \lambda(T_{n-1} + Y_n + (L-1)T_{\text{syn}} + Z_n \mathbb{I}(\text{SNR}_n \geq \Gamma))$. By the optimality equation of dynamic programming [41],

$$\begin{aligned} V(\lambda) - \lambda T_{n-1} &= \mathbb{E}[\max(U_n - \lambda T_n, V(\lambda) \\ &\quad - \lambda(T_{n-1} + Y_n + (L-1)T_{\text{syn}} + Z_n \mathbb{I}(\text{SNR}_n \geq \Gamma)))] \end{aligned} \quad (14)$$

To obtain the maximum utility $V(\lambda)$, the UE can stop searching once the currently achievable utility is not less than the

maximum expected utility that is obtained with continuing. In other words, the UE can stop searching if

$$U_n - \lambda T_n \geq V(\lambda) - \lambda(T_{n-1} + Y_n + (L-1)T_{\text{syn}} + Z_n \mathbb{I}(\text{SNR}_n \geq \Gamma)). \quad (15)$$

Adding λT_n to both sides of (15) yields that

$$U_n \geq V(\lambda) + \lambda(T_{\text{ra}} + T_{\text{data}}). \quad (16)$$

Therefore, the optimal stopping strategy for the associated ordinary optimal stopping problem is given by

$$N^*(\lambda) = \min\{n \geq 1 : U_n \geq \lambda(T_{\text{ra}} + T_{\text{data}}) + V(\lambda)\}. \quad (17)$$

Next we characterize $V(\lambda)$. Adding λT_{n-1} to both sides of (14) yields that

$$\begin{aligned} V(\lambda) &= \mathbb{E}[\max(U_n - \lambda(T_n - T_{n-1}), V(\lambda)) \\ &\quad - \lambda(Y_n + LT_{\text{syn}} + Z_n \mathbb{I}(\text{SNR}_n \geq \Gamma)))] \\ &= \mathbb{E}[\max(U_n - \lambda(T_{\text{ra}} + T_{\text{data}}), V(\lambda))] \\ &\quad - \mathbb{E}[\lambda(Y_n + (L-1)T_{\text{syn}} + Z_n \mathbb{I}(\text{SNR}_n \geq \Gamma))] \\ &= \mathbb{E}[\max(U_n - \lambda(T_{\text{ra}} + T_{\text{data}}), V(\lambda))] \\ &\quad - \lambda \left((L - \frac{1}{2})T_{\text{syn}} + \frac{T_{\text{sib}} - T_{\text{syn}}}{2} \mathbb{P}(\text{SNR}_n \geq \Gamma) \right), \end{aligned} \quad (18)$$

where we have plugged $\mathbb{E}[Y_i]$ and $\mathbb{E}[Z_i]$ (c.f. (8) and (10)) into the last equality. Rearranging the terms in (18) yields that

$$\begin{aligned} \mathbb{E}[(U_n - \lambda(T_{\text{ra}} + T_{\text{data}}) - V(\lambda))^+] \\ = \lambda \left((L - \frac{1}{2})T_{\text{syn}} + \frac{T_{\text{sib}} - T_{\text{syn}}}{2} \mathbb{P}(\text{SNR}_n \geq \Gamma) \right). \end{aligned} \quad (19)$$

By Theorem 1, Chapter 6 in [28], we know that N^* is an optimal stopping rule that attains the maximum throughput λ^* in the throughput optimization problem (5) if and only if N^* is an optimal stopping rule for the ordinary optimal stopping problem (13) with $\lambda = \lambda^*$ and $V(\lambda^*) = 0$. Plugging $V(\lambda) = 0$ into (19) yields (12). Letting $V(\lambda) = 0$ in (17) yields the optimal stopping strategy in (11).

The left side of (12) is continuous in λ and decreasing from $\mathbb{E}[U_n^+]$ to zero, while the right side of (12) is continuous in λ and increasing from 0 to $+\infty$. Hence, there is a unique solution λ^* . This completes the proof. \square

Proposition 1 implies that the optimal stopping rule is a pure threshold policy: The initial cell search and selection process stops once the maximum of the expected numbers of downlink bits of the n searched cells exceeds an optimized threshold, i.e.,

$$U_n = WT_{\text{data}} \max_{i=1, \dots, n} R_i \mathbb{I}(\text{SNR}_i \geq \Gamma) \geq \lambda^*(T_{\text{ra}} + T_{\text{data}}). \quad (20)$$

In fact, we can tighten the conclusion and show that the initial cell search and selection process can stop based on the currently examined cell only, as summarized in Proposition 2.

Proposition 2. *The optimal stopping rule for the throughput maximization problem (5) is given by*

$$N^* = \min \left\{ n \geq 1 : R_n \mathbb{I}(\text{SNR}_n \geq \Gamma) \geq \frac{\lambda^*(T_{\text{ra}} + T_{\text{data}})}{WT_{\text{data}}} \right\}, \quad (21)$$

where λ^* is the unique maximum throughput. Further, λ^* is the solution to the following fixed point equation:

$$\begin{aligned} \mathbb{E}[(WT_{\text{data}} R_n \mathbb{I}(\text{SNR}_n \geq \Gamma) - \lambda(T_{\text{ra}} + T_{\text{data}}))^+] \\ = \lambda \left((L - \frac{1}{2})T_{\text{syn}} + \frac{T_{\text{sib}} - T_{\text{syn}}}{2} \mathbb{P}(\text{SNR}_n \geq \Gamma) \right). \end{aligned} \quad (22)$$

Proof. We first claim that the rule (11) is equivalent to the rule $\hat{N} = \min\{n \geq 1 : \hat{R}_n \geq \rho\}$, where for notational simplicity we define

$$\hat{R}_n = WT_{\text{data}} R_n \mathbb{I}(\text{SNR}_n \geq \Gamma) \quad (23)$$

and $\rho = \lambda^*(T_{\text{ra}} + T_{\text{data}})$. This can be shown by induction. Clearly, at stage 1 the stopping rule (11) and \hat{N} are the same because $U_1 = \hat{R}_1$. In particular, if $U_1 = \hat{R}_1 \geq \rho$, both the rule (11) and \hat{N} call for stopping. If $U_1 = \hat{R}_1 < \rho$, both the rule (11) and \hat{N} call for continuing to stage 2. At stage 2, if $U_2 = \max(\hat{R}_1, \hat{R}_2) \geq \rho$, then $U_1 = \hat{R}_2$ because $\hat{R}_1 < \rho$ by induction. It follows that both the rule (11) and \hat{N} call for stopping. If $U_2 = \max(\hat{R}_1, \hat{R}_2) < \rho$, then $\hat{R}_2 < \rho$. Thus, both the rule (11) and \hat{N} call for continuing to stage 3. Repeating this argument for stages 3, 4, ..., we can see that the rule (11) and \hat{N} are the same stopping rules. Further, it is obvious that \hat{N} is equivalent to the rule (21).

Now we have shown that the optimal initial cell search and selection rule is to select the first cell satisfying $\hat{R}_n \geq \rho$. In particular, it is not necessary to recall any of the previously scanned cells, and the fixed point equation (22) can be derived along the same line of the proof of Proposition 1. \square

Proposition 2 implies that not only is the optimal stopping rule a pure threshold policy but also the optimal stopping is based on the currently examined cell n only, i.e.,

$$WT_{\text{data}} R_n \mathbb{I}(\text{SNR}_n \geq \Gamma) \geq \lambda^*(T_{\text{ra}} + T_{\text{data}}). \quad (24)$$

In other words, it is not necessary to recall any previously scanned cells: Simply select the cell scanned at the stopping stage N^* . This is a desirable feature in practical systems. In particular, due to e.g., the time varying radio environment, UE mobility, and clock drift, the synchronization with an earlier cell and/or the extracted cell load information might become outdated. Choosing the most recently scanned cell avoids such nuisances.

B. An Example with Binary Selection Metric

Now we have shown that the proposed initial cell search and selection scheme detailed in Section II is throughput optimal if the connection threshold μ is chosen to be $\frac{T_{\text{ra}} + T_{\text{data}}}{WT_{\text{data}}} \lambda^*$. The threshold however does not admit a closed-form solution and involves solving the fixed point equation (22). In what follows, to gain insights we consider a special case in Corollary 1 where the selection metric of each cell only takes two values.

Corollary 1. *Assume that $\text{SNR}_i \geq \Gamma, \forall i$, and that $R = R_{\text{max}}$ with probability q and $R = 0$ with probability $1 - q$. The maximum throughput λ^* is given by*

$$\lambda^* = \frac{qWT_{\text{data}}R_{\text{max}}}{(L - \frac{1}{2})T_{\text{syn}} + \frac{T_{\text{sib}} - T_{\text{syn}}}{2} + q(T_{\text{ra}} + T_{\text{data}})} \quad (25)$$

with the optimal stopping strategy given by $N^* = \min\{n \geq 1 : R_n \geq \frac{1}{1+\phi} R_{\max}\}$, where

$$\phi = \frac{(L - \frac{1}{2})T_{\text{syn}} + \frac{T_{\text{sib}} - T_{\text{syn}}}{2}}{q(T_{\text{ra}} + T_{\text{data}})}. \quad (26)$$

Several remarks on the results in Corollary 1 are in order.

Remark 1. The numerator $qWT_{\text{data}}R_{\max}$ in (25) is the expected number of information bits that UE can receive in the downlink in a communication period. The denominator in (25) is the expected duration of a communication period including the expected synchronization time $(L - \frac{1}{2})T_{\text{syn}}$, the expected time $\frac{T_{\text{sib}} - T_{\text{syn}}}{2}$ of extracting cell load information, the expected time qT_{ra} of the random access procedure, and the expected time qT_{data} of data communication. Therefore, with the optimal stopping strategy the UE makes the right decision in initial cell search and selection and achieves the optimal throughput given in (25).

Remark 2. The optimal stopping rule is a pure threshold policy: the UE stops searching and selects the currently scanned cell if $R_n/R_{\max} \geq \frac{1}{1+\phi}$. We can see that the threshold is determined by the ratio ϕ of the expected cell search time $((L - \frac{1}{2})T_{\text{syn}} + \frac{T_{\text{sib}} - T_{\text{syn}}}{2})/q$ and the expected time $T_{\text{ra}} + T_{\text{data}}$ used in the random access and data communication. Intuitively, the longer the data communication, the higher the threshold, i.e., the UE is more cautious in cell selection and is willing to search for more cells. In contrast, the longer the expected cell search time, the lower the threshold. This is because the overhead of searching for a cell becomes higher. As a result, the UE should decrease its threshold and stops earlier.

Remark 3. The maximum throughput can be written as

$$\lambda^* = \frac{1}{1+\phi} \cdot \frac{T_{\text{data}}}{T_{\text{ra}} + T_{\text{data}}} WR_{\max}, \quad (27)$$

which shows the dependency of the maximum throughput on the ratio ϕ of the expected cell search time $((L - \frac{1}{2})T_{\text{syn}} + \frac{T_{\text{sib}} - T_{\text{syn}}}{2})/q$ and the expected time $T_{\text{ra}} + T_{\text{data}}$ used in the random access and data communication. Intuitively, the higher the ratio ϕ , the lower the maximum throughput, due to the increased cell search overhead.

Remark 4. Note that the threshold of the optimal stopping (21) may not be unique, though the maximum throughput λ^* is unique. The binary selection metric taking either value R_{\max} or 0 in Corollary 1 is one such example. In particular, any value in $(0, R_{\max}]$ can be used as a threshold to achieve the maximum throughput.

C. An Alternative Characterization of the Optimal Throughput

Proposition 2 characterizes the optimal throughput via the fixed point equation (22). In this section, we derive an alternative characterization of the optimal throughput. The alternative characterization will pave the way for developing an iterative algorithm to compute the solution to the fixed point equation (22).

Denote by \hat{R} the generic random variable for $\{\hat{R}_n\}$ defined in (23) and by $F_{\hat{R}}(x)$ the cumulative distribution function of \hat{R} . The following Corollary 2 readily follows.

Corollary 2. With the throughput optimal stopping in initial cell search and selection, the following results hold.

- 1) The stopping time N^* is geometrically distributed with parameter $1 - F_{\hat{R}}(\lambda^*(T_{\text{ra}} + T_{\text{data}}))$.
- 2) The distribution of the stopped random variable U_{N^*} is given by

$$F_{U_{N^*}}(x) = \frac{F_{\hat{R}}(x) - F_{\hat{R}}(\lambda^*(T_{\text{ra}} + T_{\text{data}}))}{1 - F_{\hat{R}}(\lambda^*(T_{\text{ra}} + T_{\text{data}}))} \quad (28)$$

with $x \geq \lambda^*(T_{\text{ra}} + T_{\text{data}})$.

Proof. From Proposition 2, we know that UE stops searching and selects cell n if $\hat{R}_n \geq \lambda^*(T_{\text{ra}} + T_{\text{data}})$. It follows that the number N^* of searched cells is geometrically distributed with parameter $1 - F_{\hat{R}}(\lambda^*(T_{\text{ra}} + T_{\text{data}}))$. At the throughput optimal stopping time N^* , $U_{N^*} = \hat{R}_{N^*}$. Further, the distribution of \hat{R}_{N^*} is a conditional distribution that results from restricting the domain of the distribution \hat{R} to $x \geq \lambda^*(T_{\text{ra}} + T_{\text{data}})$. This completes the proof. \square

With Corollary 2, we are now in a position to derive the alternative characterization of the optimal throughput in the following Proposition 3.

Proposition 3. With the throughput optimal stopping in initial cell search and selection, the maximum throughput λ^* is given by

$$\lambda^* = \frac{\int_{\lambda^*(T_{\text{ra}} + T_{\text{data}})}^{\infty} x \, dF_{\hat{R}}(x)}{\eta + (T_{\text{ra}} + T_{\text{data}})(1 - F_{\hat{R}}(\lambda^*(T_{\text{ra}} + T_{\text{data}})))}, \quad (29)$$

where $\eta \triangleq (L - \frac{1}{2})T_{\text{syn}} + \frac{1}{2}(T_{\text{sib}} - T_{\text{syn}})\mathbb{P}(\text{SNR} \geq \Gamma)$.

Proof. By Lemma 1, we have

$$\begin{aligned} \mathbb{E}[T_{N^*}] &= \mathbb{E}[N^*] \left(L - \frac{1}{2} \right) T_{\text{syn}} \\ &+ \frac{\mathbb{E}[N^*]}{2} (T_{\text{sib}} - T_{\text{syn}}) \mathbb{P}(\text{SNR} \geq \Gamma) + T_{\text{ra}} + T_{\text{data}}. \end{aligned} \quad (30)$$

By the first result in Corollary 2, we have

$$\mathbb{E}[N^*] = \frac{1}{1 - F_{\hat{R}}(\lambda^*(T_{\text{ra}} + T_{\text{data}}))}. \quad (31)$$

By the second result in Corollary 2, we have

$$\begin{aligned} \mathbb{E}[U_{N^*}] &= \int_{\lambda^*(T_{\text{ra}} + T_{\text{data}})}^{\infty} x \, dF_{U_{N^*}}(x) \\ &= \frac{1}{1 - F_{\hat{R}}(\lambda^*(T_{\text{ra}} + T_{\text{data}}))} \int_{\lambda^*(T_{\text{ra}} + T_{\text{data}})}^{\infty} x \, dF_{\hat{R}}(x). \end{aligned} \quad (32)$$

Plugging (30), (31), and (32) into $\lambda^* = \frac{\mathbb{E}[U_{N^*}]}{\mathbb{E}[T_{N^*}]}$ yields (29). \square

Proposition 3 provides an alternative fixed point equation (29) whose solution is the maximum throughput. It also suggests one possible numerical iterative algorithm to solve for λ^* . Denote by t the iteration index. Replacing the λ^* on the left hand side of (29) by $\lambda[t+1]$ and the λ^* on the right hand side of (29) by $\lambda[t]$ yields that

$$\lambda[t+1] = \frac{\int_{\lambda[t](T_{\text{ra}} + T_{\text{data}})}^{\infty} x \, dF_{\hat{R}}(x)}{\eta + (T_{\text{ra}} + T_{\text{data}})(1 - F_{\hat{R}}(\lambda[t](T_{\text{ra}} + T_{\text{data}})))}. \quad (33)$$

This iterative method is in essence a variation of Newton's method with all iterations using a unit step size. The following Proposition 4 formally establishes the convergence of the iterative equation (33).

Proposition 4. *For any initial value $\lambda[0] > 0$, the sequence $\{\lambda[t]\}$ generated by the iterative equation (33) converges to the maximum throughput λ^* .*

Proof. For notational simplicity, denote by

$$h(z) = \frac{\int_{z(T_{ra}+T_{data})}^{\infty} x \, dF_{\hat{R}}(x)}{\eta + (T_{ra} + T_{data})(1 - F_{\hat{R}}(z(T_{ra} + T_{data})))}. \quad (34)$$

By definition, $h(0) > 0$, $\lambda^* = \max_{\lambda} h(\lambda)$, and λ^* is the unique maximum value. It follows that $\lambda \leq h(\lambda)$ if $\lambda \leq \lambda^*$, and $\lambda > h(\lambda)$ if $\lambda > \lambda^*$. For any initial value $\lambda[0] > 0$, if $\lambda[0] > \lambda^*$, $\lambda[0] > h(\lambda[0]) = \lambda[1]$. Since $\lambda[1] \leq \lambda^*$, we may assume without loss of generality that $\lambda[0] \leq \lambda^*$. Further, we have $\lambda[0] \leq h(\lambda[0]) = \lambda[1]$ and $h(\lambda[0]) \leq h(\lambda^*) = \lambda^*$. It follows that $\lambda[0] \leq \lambda[1] \leq \lambda^*$. By induction, it can be seen that $\{\lambda[t]\}$ is monotonically non-decreasing and is bounded by λ^* . Therefore, $\{\lambda[t]\}$ converges to some limiting point λ_{∞} . In particular,

$$\begin{aligned} 0 &= \lim_{t \rightarrow \infty} (\lambda[t+1] - \lambda[t]) \\ &= \lim_{t \rightarrow \infty} \left(\frac{\int_{\lambda[t](T_{ra}+T_{data})}^{\infty} x \, dF_{\hat{R}}(x)}{\eta + (T_{ra} + T_{data})(1 - F_{\hat{R}}(\lambda[t](T_{ra} + T_{data})))} - \lambda[t] \right) \\ &= \frac{\int_{\lambda_{\infty}(T_{ra}+T_{data})}^{\infty} x \, dF_{\hat{R}}(x)}{\eta + (T_{ra} + T_{data})(1 - F_{\hat{R}}(\lambda_{\infty}(T_{ra} + T_{data})))} - \lambda_{\infty}. \end{aligned} \quad (35)$$

It follows that

$$\lambda_{\infty} = \frac{\int_{\lambda_{\infty}(T_{ra}+T_{data})}^{\infty} x \, dF_{\hat{R}}(x)}{\eta + (T_{ra} + T_{data})(1 - F_{\hat{R}}(\lambda_{\infty}(T_{ra} + T_{data})))}. \quad (36)$$

In other words, λ_{∞} is also the solution to the fixed point equation (8) whose solution is the maximum throughput λ^* . Since the solution is unique, we must have $\lambda_{\infty} = \lambda^*$. \square

V. SIMULATION RESULTS

In this section, we provide simulation results to demonstrate the analytical results and obtain insights into how the various system parameters affect the throughput optimal initial cell search and selection. In the simulation, the load value broadcast by each cell i is $\beta_i = \frac{1}{M_i+1}$, where recall M_i is the number of active UEs served by BS i . The received SNR from BS i equals $\text{SNR}_i = g \cdot L \cdot \text{SNR}_{\text{avg}}$, where g models log-normal shadowing and L models the beamforming gain. The specific parameters used are summarized in Table I unless otherwise specified.

Figure 2 shows a sample trace of initial cell search and selection. As the number n of searched cells increases, the cell search time T_n increases. Note that the cell search time T_n is not a simple linear function of the number n of searched cells (though visually a linear relationship is shown in Figure 2). In particular, the cell search of each cell may consist of two parts: synchronization and cell load information reading. If the received SNR is below the threshold Γ , UE does not proceed with reading the load information after synchronization. The

Mean # of active UEs per cell M_i	10
Std. dev. of log-normal shadowing	7 dB
# of beamforming pairs L	64
Average received SNR SNR_{avg}	-10 dB
SNR threshold Γ	-10 dB
Syn. signals period T_{syn}	0.005 s
System info. period T_{sib}	0.01 s
Random access time T_{ra}	0.02 s
Data communication time T_{data}	10 s
Channel bandwidth W	1 GHz

TABLE I
SIMULATION PARAMETERS

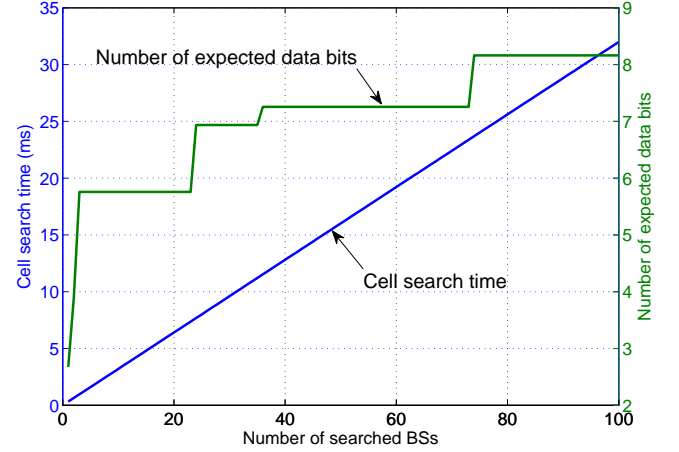


Fig. 2. A sample trace of initial cell search and selection.

exact relationship is given in (2) excluding the last two terms T_{ra} and T_{data} . Figure 2 also shows that the amount of downlink bits that UE may expect to receive is a non-decreasing function of the number n of searched cells, which is intuitive. To sum up, Figure 2 illustrates the tradeoff in searching for more cells in initial cell search and selection: Scanning more cells increases the probability of finding a better cell but at the cost of more overhead time spent on cell search.

In Figure 3, we study how the throughput performance varies with the stopping selection metric threshold R_i under different numbers L of beamforming pairs. The data communication time is $T_{\text{data}} = 10$ s, and the mean number of active UEs per cell equals 10. For each number of beamforming pairs, Figure 3 clearly shows that there exists an optimal stopping threshold that achieves the maximum throughput. The maximum throughput increases when the number of beamforming pairs increases from 4 to 16 and to 64, but it decreases when the number of beamforming pairs increases from 64 to 256. This is because there is a tradeoff when increasing the number of beamforming pairs. One the one hand, increasing the number of beamforming pairs increases the beamforming gain and in turn improves the received SNR. On the other hand, increasing the number of beamforming pairs also increases the synchronization time spent on cell search since more beamforming pairs need to be scanned.

From Figure 3, we can see that the optimal stopping selection metric threshold increases noticeably when the number of

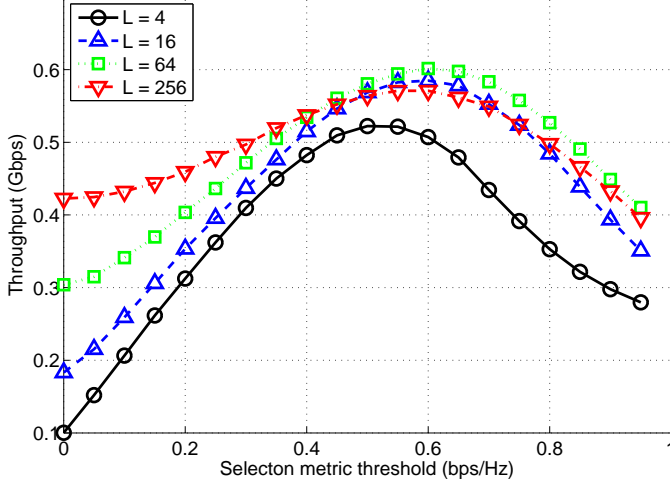


Fig. 3. Ergodic throughput versus selection metric threshold under different numbers L of beamforming pairs: $T_{\text{data}} = 10$ s; mean number of active UEs per cell equals 10.

beamforming pairs increases from 4 to 16. So does the maximum throughput. This suggests that in this regime increasing beamforming gain is quite instrumental and much outweighs the cost of more time spent in cell search. In particular, UE can afford to search for more cells before camping on a cell and thus can set a higher stopping selection metric threshold. In contrast, when the number of beamforming pairs increases from 16 to 64 and to 256, the optimal stopping selection metric threshold stays almost invariant and the maximum throughput does not change much. This suggests that in this regime the benefit from increasing the beamforming gain becomes saturated and is also offset by the increased overhead time in cell search.

In Figure 4, the setup is the same as in Figure 3 except that the data communication time is increased by 4 times to 40 s. Comparing Figure 4 to Figure 3, we can see that for each number L of beamforming pairs, the maximum throughput with $T_{\text{data}} = 40$ s in Figure 4 is larger than its corresponding part with $T_{\text{data}} = 10$ s in Figure 3. This agrees with intuition: As the data communication time increases, the relative time overhead of cell search and random access becomes smaller, resulting in higher throughput. Further, for each number L of beamforming pairs, the optimal selection metric threshold with $T_{\text{data}} = 40$ s in Figure 4 is larger than its counterpart with $T_{\text{data}} = 10$ s in Figure 3. This is because the relative time overhead of cell search becomes smaller as the data communication time increases. As a result, UE can set a higher stopping selection metric threshold to search for more cells before camping on a cell.

In Figure 5, the setup is the same as in Figure 3 except that the mean number of active UEs per cell is decreased by 2 times to 5. Since $\beta_i = \frac{1}{M_i+1}$, the expected scheduling probability of each cell i is statistically larger in Figure 5 than in Figure 3. In other words, the load in Figure 5 is statistically lighter than in Figure 3. Comparing Figure 5 to Figure 3, we can see that the throughput values in Figure 5 are about twice as

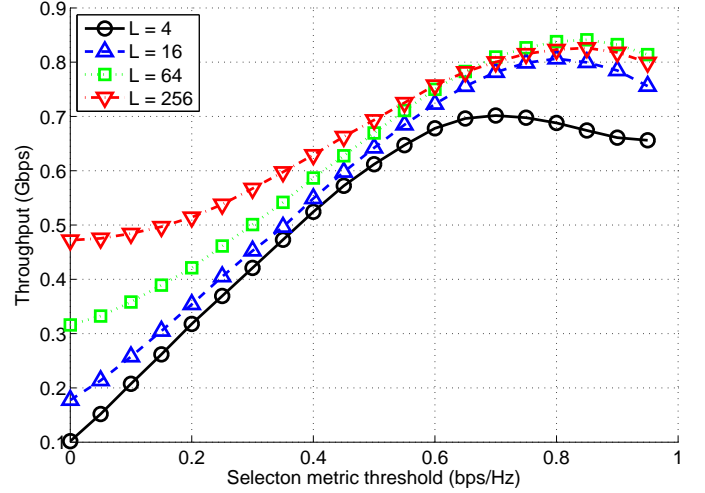


Fig. 4. Ergodic throughput versus selection metric threshold under different numbers L of beamforming pairs: $T_{\text{data}} = 40$ s; mean number of active UEs per cell equals 10.

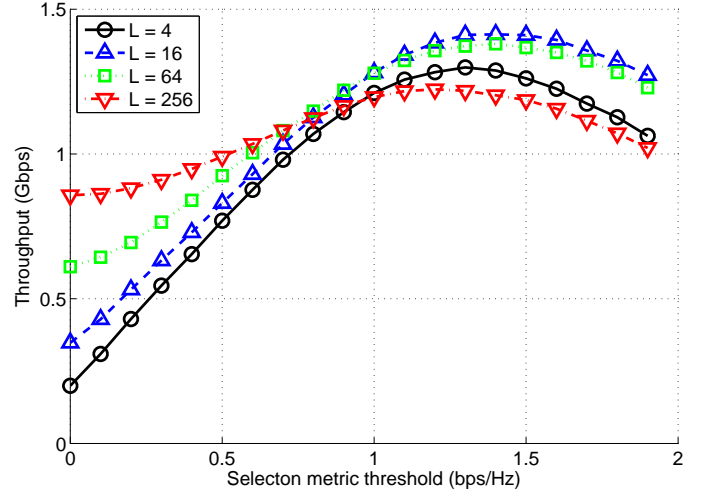


Fig. 5. Ergodic throughput versus selection metric threshold under different numbers L of beamforming pairs: $T_{\text{data}} = 10$ s; mean number of active UEs per cell equals 5.

large as their counterparts in Figure 3, agreeing with intuition. Accordingly, for each number L of beamforming pairs, the optimal selection metric threshold in Figure 4 is larger than its counterpart in Figure 3. One interesting observation is that in Figure 5 the maximum throughput with $L = 16$ is larger than the maximum throughput with $L = 64$. The converse is true in Figure 3. This suggests beamforming gain is more instrumental in improve the throughput performance when the load is heavier. When the load is light, the throughput values are high since UE has access to more radio resources, and thus the beamforming gain becomes less important.

In Figure 3, Figure 4, or Figure 5, it can be observed that the throughput performance becomes less sensitive when the numbers L of beamforming pairs increases. This is because as the number L of beamforming pairs increases, the radio

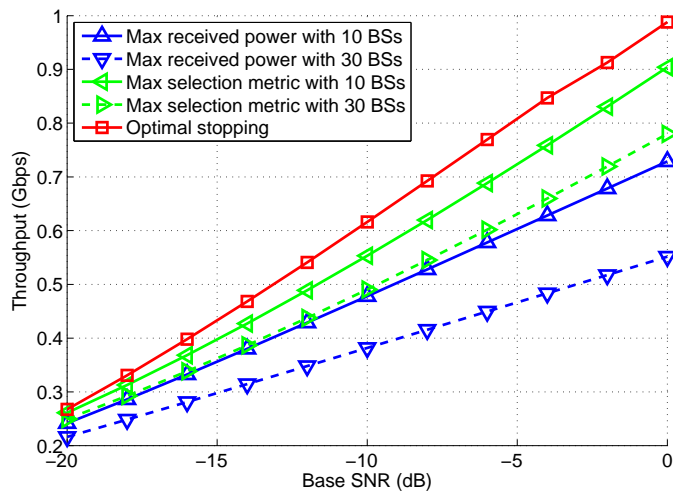


Fig. 6. Comparison of throughput performance under different cell search and selection strategies.

channels become “hardened” and the relative variation of the received SNR reduces. As a result, less opportunism may be exploited by choosing an optimized selection threshold.

In Figure 6, we compare the throughput performance attained by the proposed cell search and selection scheme with optimal stopping to the performance of several other cell search and selection strategies. The first scheme is the max-received-power association, where UE scans a number of cells and then selects the one that yields the maximum received power. The second scheme is to scan a *fixed* number of cells and then selects the one that yields the largest selection metric. For either the max-received-power association or the max-selection-metric association, we consider two values for the number of searched BSs in Figure 6: 10 and 30. Figure 6 shows that the max-received-power association has the worst performance since it only takes into account the received power but ignores the important load factor. The max-selection-metric association takes into account both the received power and the load, but its stopping strategy of searching a fixed number of BSs is suboptimal. The throughput performance is optimized when the association is based on the proposed selection metric combined with the derived optimal stopping rule.

VI. CONCLUSIONS

Careful design and optimization in every aspect of 5G networks is needed to facilitate the adoption of 5G in the IoT. In this paper, we have studied initial cell search and selection in 5G millimeter wave networks. We propose a load aware initial cell search and selection scheme, which is simple yet powerful. It equips the networks with a powerful access control method that facilitates load balancing. We also formulate a throughput optimization problem using the optimal stopping theory. We characterize the throughput optimal stopping strategy and the attained maximum throughput. The results show that the proposed initial cell search and selection scheme

is throughput optimal with a carefully optimized connection threshold.

This work can be extended in a number of ways. The selection metric investigated in this paper is a function of SNR. One may consider extending this metric to incorporate the effect of interference. Collisions in random access that is part of initial access procedure are not considered in this paper. It will be of interest to explore the impact of collisions on the performance.

REFERENCES

- [1] X. Lin, J. Li, R. Baldemair, T. Cheng, S. Parkvall, D. Larsson, H. Koorapaty, M. Frenne, S. Falahati, A. Grövlén *et al.*, “5G new radio: Unveiling the essentials of the next generation wireless access technology,” *arXiv preprint arXiv:1806.06898*, June 2018.
- [2] M. S. Omar, S. A. Hassan, H. Pervaiz, Q. Ni, L. Musavian, S. Mumtaz, and O. A. Dobre, “Multiobjective optimization in 5G hybrid networks,” *IEEE Internet of Things Journal*, vol. 5, no. 3, pp. 1588–1597, June 2018.
- [3] W. Ejaz and M. Ibnkahla, “Multi-band spectrum sensing and resource allocation for IoT in cognitive 5G networks,” *IEEE Internet of Things Journal*, vol. 5, no. 1, pp. 150–163, February 2018.
- [4] E. Dahlman, S. Parkvall, and J. Skold, *4G: LTE/LTE-advanced for mobile broadband*. Academic press, 2013.
- [5] 3GPP, “Evolved universal terrestrial radio access (E-UTRA); user equipment (UE) procedures in idle mode,” *3GPP TS 36.304 V14.0.0*, September 2016.
- [6] X. Lin, A. Adhikary, and Y.-P. E. Wang, “Random access preamble design and detection for 3GPP narrowband IoT systems,” *IEEE Wireless Communications Letters*, vol. 5, no. 6, pp. 640–643, December 2016.
- [7] J. G. Andrews, S. Singh, Q. Ye, X. Lin, and H. S. Dhillon, “An overview of load balancing in HetNets: Old myths and open problems,” *IEEE Wireless Communications*, vol. 21, no. 2, pp. 18–25, April 2014.
- [8] N. Bhushan, J. Li, D. Malladi, R. Gilmore, D. Brenner, A. Damjanovic, R. T. Sukhvasi, C. Patel, and S. Geirhofer, “Network densification: the dominant theme for wireless evolution into 5G,” *IEEE Communications Magazine*, vol. 52, no. 2, pp. 82–89, February 2014.
- [9] J. G. Andrews, S. Buzzi, W. Choi, S. V. Hanly, A. Lozano, A. C. Soong, and J. C. Zhang, “What will 5G be?” *IEEE Journal on Selected Areas in Communications*, vol. 32, no. 6, pp. 1065–1082, June 2014.
- [10] T. Rappaport, S. Sun, R. Mayzus, H. Zhao, Y. Azar, K. Wang, G. Wong, J. Schulz, M. Samimi, and F. Gutierrez, “Millimeter wave mobile communications for 5G cellular: It will work!” *IEEE Access*, vol. 1, pp. 335–349, May 2013.
- [11] S. Singh, F. Ziliotto, U. Madhow, E. Belding, and M. Rodwell, “Blockage and directivity in 60GHz wireless personal area networks: From cross-layer model to multihop MAC design,” *IEEE Journal on Selected Areas in Communications*, vol. 27, no. 8, pp. 1400–1413, October 2009.
- [12] X. Lin and J. G. Andrews, “Connectivity of millimeter wave networks with multi-hop relaying,” *IEEE Wireless Communications Letters*, vol. 4, no. 2, pp. 209–212, February 2015.
- [13] J. Lu, D. Steinbach, P. Cabrol, and Pietraski, “Modeling the impact of human blockers in millimeter wave radio links,” *ZTE Communications Magazine*, vol. 10, no. 4, pp. 23–28, December 2012.
- [14] C. N. Barati, S. A. Hosseini, S. Rangan, P. Liu, T. Korakis, S. S. Panwar, and T. S. Rappaport, “Directional cell discovery in millimeter wave cellular networks,” *IEEE Transactions on Wireless Communications*, vol. 14, no. 12, pp. 6664–6678, December 2015.
- [15] C. N. Barati, S. A. Hosseini, M. Mezzavilla, T. Korakis, S. S. Panwar, S. Rangan, and M. Zorzi, “Initial access in millimeter wave cellular systems,” *IEEE Transactions on Wireless Communications*, vol. 15, no. 12, pp. 7926–7940, December 2016.
- [16] H. Shokri-Ghadikolaei, C. Fischione, G. Fodor, P. Popovski, and M. Zorzi, “Millimeter wave cellular networks: A MAC layer perspective,” *IEEE Transactions on Communications*, vol. 63, no. 10, pp. 3437–3458, 2015.
- [17] V. Raghavan, J. Cezanne, S. Subramanian, A. Sampath, and O. Koymen, “Beamforming tradeoffs for initial ue discovery in millimeter-wave MIMO systems,” *IEEE Journal of Selected Topics in Signal Processing*, vol. 10, no. 3, pp. 543–559, March 2016.

- [18] M. Giordani, M. Mezzavilla, C. N. Barati, S. Rangan, and M. Zorzi, "Comparative analysis of initial access techniques in 5G mmwave cellular networks," in *Proceedings of the Annual Conference on Information Science and Systems (CISS)*, 2016, pp. 268–273.
- [19] F. Ahmed, J. Deng, and O. Tirkkonen, "Self-organizing networks for 5G: Directional cell search in mmw networks," in *IEEE Personal, Indoor, and Mobile Radio Communications (PIMRC)*, 2016, pp. 1–5.
- [20] I. Filippini, V. Sciancalepore, F. Devoti, and A. Capone, "Fast cell discovery in mm-wave 5G networks with context information," *IEEE Transactions on Mobile Computing*, vol. 17, no. 7, pp. 1538–1552, July 2018.
- [21] Y. Li, J. G. Andrews, F. Baccelli, T. D. Novlan, and C. J. Zhang, "Design and analysis of initial access in millimeter wave cellular networks," *IEEE Transactions on Wireless Communications*, vol. 16, no. 10, pp. 6409–6425, October 2017.
- [22] X. Lin, J. G. Andrews, and A. Ghosh, "Modeling, analysis and design for carrier aggregation in heterogeneous cellular networks," *IEEE Transactions on Communications*, vol. 61, no. 9, pp. 4002–4015, September 2013.
- [23] A. Damnjanovic, J. Montojo, Y. Wei, T. Ji, T. Luo, M. Vajapeyam, T. Yoo, O. Song, and D. Malladi, "A survey on 3GPP heterogeneous networks," *IEEE Wireless Communications*, vol. 18, no. 3, pp. 10–21, March 2011.
- [24] Q. Ye, B. Rong, Y. Chen, M. Al-Shalash, C. Caramanis, and J. G. Andrews, "User association for load balancing in heterogeneous cellular networks," *IEEE Transactions on Wireless Communications*, vol. 12, no. 6, pp. 2706–2716, June 2013.
- [25] E. Aryafar, A. Keshavarz-Haddad, M. Wang, and M. Chiang, "RAT selection games in HetNets," in *Proceedings of the IEEE INFOCOM*, 2013, pp. 998–1006.
- [26] T. K. Vu, M. Bennis, S. Samarakoon, M. Debbah, and M. Latva-aho, "Joint load balancing and interference mitigation in 5G heterogeneous networks," *IEEE Transactions on Wireless Communications*, vol. 16, no. 9, pp. 6032–6046, September 2017.
- [27] G. Peskir and A. Shiryaev, *Optimal stopping and free-boundary problems*. Springer, 2006.
- [28] T. S. Ferguson, "Optimal stopping and applications," 2012. Available at <http://www.math.ucla.edu/~tom/Stopping/Contents.html>.
- [29] P. Chaporkar and A. Proutiere, "Optimal joint probing and transmission strategy for maximizing throughput in wireless systems," *IEEE Journal on Selected Areas in Communications*, vol. 26, no. 8, pp. 1546–1555, October 2008.
- [30] D. Zheng, W. Ge, and J. Zhang, "Distributed opportunistic scheduling for ad hoc networks with random access: An optimal stopping approach," *IEEE Transactions on Information Theory*, vol. 55, no. 1, pp. 205–222, January 2009.
- [31] H. Jiang, L. Lai, R. Fan, and H. V. Poor, "Optimal selection of channel sensing order in cognitive radio," *IEEE Transactions on Wireless Communications*, vol. 8, no. 1, pp. 297–307, January 2009.
- [32] Y. J. Zhang, "Multi-round contention in wireless LANs with multipacket reception," *IEEE Transactions on Wireless Communications*, vol. 9, no. 4, pp. 1503–1513, April 2010.
- [33] H. T. Cheng and W. Zhuang, "Simple channel sensing order in cognitive radio networks," *IEEE Journal on Selected Areas in Communications*, vol. 29, no. 4, pp. 676–688, April 2011.
- [34] M. I. Poulakis, A. D. Panagopoulos, and P. Constantinou, "Channel-aware opportunistic transmission scheduling for energy-efficient wireless links," *IEEE Transactions on Vehicular Technology*, vol. 62, no. 1, pp. 192–204, January 2013.
- [35] G. Yang, C. K. Ho, and Y. L. Guan, "Dynamic resource allocation for multiple-antenna wireless power transfer," *IEEE Transactions on Signal Processing*, vol. 62, no. 14, pp. 3565–3577, July 2014.
- [36] N. Wei, X. Lin, and Z. Zhang, "Optimal relay probing in millimeter-wave cellular systems with device-to-device relaying," *IEEE Transactions on Vehicular Technology*, vol. 65, no. 12, pp. 10 218–10 222, December 2016.
- [37] H. Li, C. Huang, P. Zhang, S. Cui, and J. Zhang, "Distributed opportunistic scheduling for energy harvesting based wireless networks: A two-stage probing approach," *IEEE/ACM Transactions on Networking*, vol. PP, no. 99, pp. 1–14, 2015.
- [38] A. S. Cacciapuoti, M. Caleffi, and L. Paura, "Optimal strategy design for enabling the coexistence of heterogeneous networks in tv white space," *IEEE Transactions on Vehicular Technology*, vol. 65, no. 9, pp. 7361–7373, September 2016.
- [39] N. Wei, X. Lin, W. Li, Y. Xiong, and Z. Zhang, "Throughput optimal listen-before-talk for cellular in unlicensed spectrum," in *IEEE International Conference on Communications (ICC)*, May 2017, pp. 1–6.
- [40] 3GPP, "Evolved universal terrestrial radio access (E-UTRA); radio resource control (RRC); protocol specification," *3GPP TS 36.331 V14.0.0*, October 2016.
- [41] D. P. Bertsekas, *Dynamic programming and optimal control*. Athena Scientific Belmont, MA, 1995, vol. 1, no. 2.